Sensors and Materials, Vol. 17, No. 1 (2005) 039–048
MYU Tokyo

S & M 0584

Characteristics of Anodic-Bonded Multilayer Ceramic Actuators on Si Wafers for MEMS Applications

Gwiy-Sang Chung

Department of Mechatronics Engineering, Dongseo University,
San 69-1, Churye-Dong, Sasang-Gu, Busan 617-716, Korea

(Received September 22, 2004; accepted November 5, 2004)

Key words: anodic bonding, multilayer ceramic actuators, Pyrex #7740 glass, MEMS

This paper describes the characteristics of anodic-bonded multilayer ceramic actuators (MCA) on Si wafers using sputtered Pyrex #7740 glass thin films for micro-electromechanical-system (MEMS) applications. The Pyrex #7740 glass thin films were deposited on MCA under optimum RF magnetron conditions ($Ar:O_2$ gas ratio of 100%, input power of 1 W/cm^2). After annealing at 450°C for 1 h, the anodic bonding of MCA to a Si wafer was successfully performed at 600 V, at 400°C and –760 mmHg. The properties of the MCA/Si bonded interface and fabricated Si diaphragm deflection were analyzed through the actuation test. It is possible to control with accuracy the deflection of a Si diaphragm according to its geometry; here, a maximum nonlinearity of 0.05–0.08% FS was observed. Moreover, no damage or separation of MCA/Si bonded interfaces occurred during the actuation test. Therefore, it is expected that anodic bonding technology of MCA/Si wafers could be usefully applied to the fabrication process of high-performance piezoelectric MEMS devices.

I. Introduction

Piezoelectric ceramics are being widely used to fabricate micro-electromechanical-system (MEMS) devices with high performances, as well as electronic devices, such as FRAM and transducer applications. Particularly, they have several advantages, such as a larger generative force, quicker response and smaller drive voltage than devices utilizing electrostatic, electromagnetic and pneumatic forces. Additionally, much research is being carried out into using piezoelectric ceramics for micro-control units, such as medical drug delivery systems and chemical analysis systems.[1]

*Corresponding author, e-mail address: gschung@dongseo.ac.kr

Recently, these fabricated MEMS devices using piezoelectric thin film ceramics have been employed as a driving principle because of their properties such as small size, high response, low power consumption and large driving force *et al.* However, piezoelectric thin film ceramics have a number of problems, such as insufficient driving forces and response time and a high resonance frequency. Therefore, in the future, it is expected that multilayer ceramic actuators (MCA) will be substituted for piezoelectric thin film ceramics for use as the actuating parts of MEMS devices with good thermal loss quality, displacement accuracy and low power consumption.[2]

Currently, MCA and Si wafer bonding techniques are important for maintaining the electric-mechanical coupling factor and enabling the formation of a perfect bond without a nonbonded area. Organic adhesive materials (*e.g.*, epoxy resin) have been mainly used when the MCA/Si wafer bonding process is performed. However, the adhesive materials used in the bonding process have their inherent disadvantage; it is impossible or extremely difficult to control the thickness of the adhesive materials and the bond strength is variable according to the rate of hardening. Meanwhile, the anodic bonding of a Si wafer to glass is required for many MEMS devices (typically Pyrex #7740 is used), which have dielectric characteristics. The several advantages of anodic bonding have been previously reported in a number of papers.[3–5] Anodic bonding can be used at low temperatures of below 500°C, and the heat resistance and reliable bond strength (approximately more than 350 psi) of a bonded sample are larger than those obtained by other methods.

The aim of this work is to analyze the anodic bonding characteristics between MCA and a Si wafer, and to develop high-performance MEMS devices without deterioration of bond characteristics. In order to succeed in the MCA/Si wafer anodic bonding with electrostatic forces, the deposition of Pyrex #7740 glass thin films is very important. Thus, in this work, a Pyrex #7740 glass thin film was formed on a MCA surface under various RF sputtering conditions, and the surface roughness and composition ratio of the glass thin films was analyzed by atomic force microscopy (AFM), X-ray photoelectron spectroscopy (XPS) and with a profilometer, respectively. Subsequently, the optimum RF sputtering conditions for depositing Pyrex #7740 glass were determined. Finally, after the bonding process, we evaluated the cross-sectional image of the anodic-bonded MCA/Si wafer obtained by scanning electron microscopy (SEM), and demonstrated actuation characteristics with laser displacement sensors for MEMS applications.

2. Experiments

2.1 *Glass thin film deposition*

Sodium-containing Pyrex #7740 glass was deposited on a MCA surface by RF sputtering. In the case of anodic bonding via an intermediate glass layer, it is important that the properties of the formed glass thin films such as thermal expansion coefficient, sodium content and surface roughness are the same those of the Pyrex #7740 glass targets. First, we analyzed the characteristics of Pyrex glass thin films as a function of sputtering conditions. After the glass thin film deposition with the addition of oxygen (0–40 % $Ar:O_2$ gas ratio) and increasing input power (1–3 W/cm^2), the sputtered glass thin films were annealed at 450°C for 60 min to reduce residual stress.[6] The optimum RF sputtering

conditions of Pyrex glass thin film deposition were determined by XPS, AFM, and with profilometer. Table 1 shows the RF sputtering and annealing conditions.

2.2 *Anodic bonding*

A boron-doped P(100) Si wafer with dimensions of 2×2 cm^2 and a thickness of 510 μm, and a 5000 Å-thick glass thin film deposited on a MCA (5×5×20 mm^3) were cleaned before anodic bonding. First, to maintain the hydrophilic property, the Si substrates were subjected to a standard semiconductor cleaning process to remove organic/inorganic particles using HCl, H_2SO_4 and buffered HF (BHF). In addition, the glass thin films on the MCA are ultrasonically cleaned using microsoap, trichloroethylene (TCE) and isopropyl alcohol (IPA).

Using conventional anodic bonding equipment, the glass layer on the MCA and the polished Si wafer were placed next to the cathode and the anode on the heater plate, respectively. Under the bonding conditions of 600 V and 400°C, the samples of the MCA and the Si substrate were subjected to the bonding process in the anodic chamber for 60 min. Finally, we evaluated the interface characteristics between glass and Si, and also analyzed the bonding strength after anodic bonding in the vacuum chamber.

3. Results and Discussion

3.1 *Evaluation of sputtered glass thin films*

Pyrex #7740 glass as a sputter target is mainly composed of 81% SiO_2, 13% B_2O_3, 2.5% Na_2O, 2% Al_2O_3, 0.6% K_2O and others < 0.9%. The composition of the glass thin films deposited by sputtering is evaluated by XPS analysis. For an Ar:O_2 gas ratio of 100%, sodium content increased to approximately 1.7% as shown in Fig. 1. However, in the range of 10–40 % Ar:O_2 gas ratio, sodium content decreased by 0.913–1.262%. We also evaluated a glass thin film on MCA with increasing RF power density (1–3 W/cm^2). With decreasing RF power density, the sodium content was increased from 0.96% to 1.30%.

Figure 2 shows the etch-rate characteristics of the deposited glass thin films using BHF ($HF+NH_4F+H_2O$=30 ml/20 g/200 ml) after annealing at 450°C for 60 min. In general, silica ions are very strongly bonded to oxygen. In the case of the sputtered Pyrex #7740

Table 1
RF sputtering and annealing conditions of Pyrex #7740 glass.

Method	RF sputtering
Target	Pyrex #7740 glass
RF power density	1–3 W/cm^2
Sputter gas	Ar-(0–40%)O_2
Base pressure	2×10^{-5} Torr
Working pressure	4×10^{-3} Torr
Deposition rate	0.1 μm/h
Substrate temperature	Room temp.
Annealing conditions	400°C, 1 h

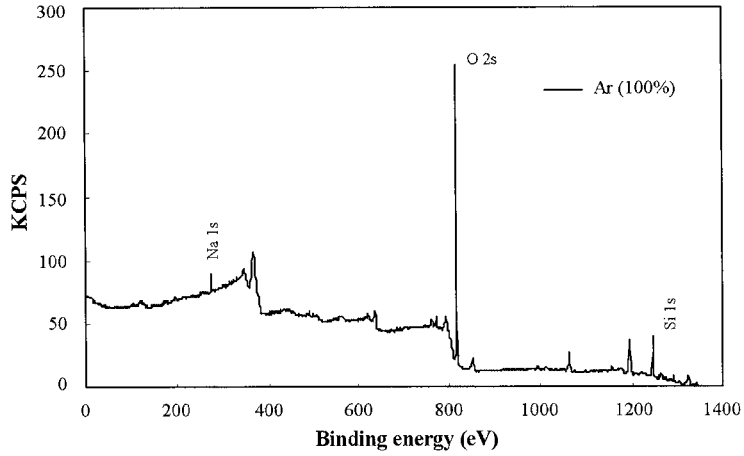

Fig. 1. XPS Analysis of sputtered Pyrex #7740 glass thin films under conditions: Ar 100%, 1.0 W/cm^2.

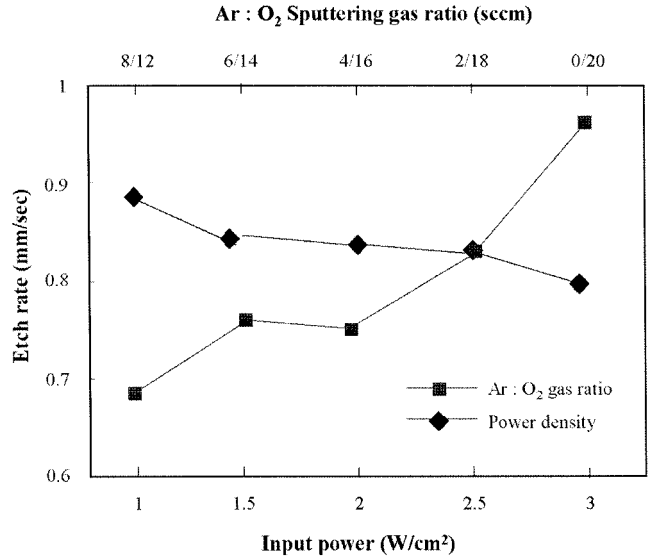

Fig. 2. Etch rates of deposited Pyrex #7740 glass thin films versus sputtering gas ratio and input power.

glass, which has a large percentage of silica ions, diffusion of the etchant occurs at high rates.[7] In our experimental results, with increasing Ar sputtering gas ratio, the etch rate of the deposited glass increased to 970 Å/min. Additionally, the etch rates of the deposited glass thin films for various input powers were measured. With reduced input power density, the etch rate was observed to increase. These etch-rate characteristics agree with the above-mentioned XPS analysis. From these results, it is confirmed that RF sputtering with an Ar:O_2 gas ratio of 100% and input power density of 1 W/cm^2 results in a film with higher sodium content than with other Ar:O_2 gas ratios and input powers, and minimizes the change in thermal expansion coefficient of Pyrex #7740 glass.

The surface roughness of deposited glass has a decisive effect on bond strength. The surface roughness of glass thin films deposited at different input power densities was evaluated by AFM. With decreasing input power from 3 to 1 W/cm^2, surface roughness was reduced to 31 Å. Therefore, as stated in the above results, an Ar:O_2 gas ratio of 100% and an input power of 1 W/cm^2 are selected as the optimum RF sputtering conditions for the Pyrex glass thin film deposition, and Pyrex #7740 glass is deposited onto a MCA for anodic bonding.

3.2 *Anodic bonding characteristics*

In this work, the bonding process of the MCA and the hydrophilic Si substrate, was performed at 400°C, at 600 V for 1 h. Figure 3 shows the SEM image of the successfully anodic-bonded MCA/Si wafer interface using sputtered Pyrex #7740 glass thin films for MEMS applications. It is confirmed that the MCA/Si wafer samples are perfectly bonded by the electrostatic forces without the presence of nonbonded surface. Also, anodic bonding is successful for a glass thickness of at least 5000 Å, because surface roughness decreases with increasing glass thickness. Thus, in the case of using Pyrex #7740 glass thin films as an intermediate layer during the anodic bonding of MCA to a Si wafer, the deposition of glass thin films with a minimum thickness of 5000 Å is necessary to improve the glass surface roughness.

3.3 *Application to MEMS*

In the case of the perfectly bonded sample, the poling treatment is performed in silicon oil with a 30 kV/cm^2 applied voltage at 100°C for 10 min. Finally, the reliability of anodic bonding is evaluated through the actuation test and simulation of the MCA/Si bonded sample. The goal of this experiment and simulation is to determine the Si diaphragm dimensions and apply the fabricated actuating part to devices, such as a microvalve, a micropump and an injection printer with accurate deflection control. After the UV photolithography process, the bonded Si wafer is anisotropic etched in tetra-methyl ammonium hydroxide (TMAH) solution of 20 wt.% at 80°C.

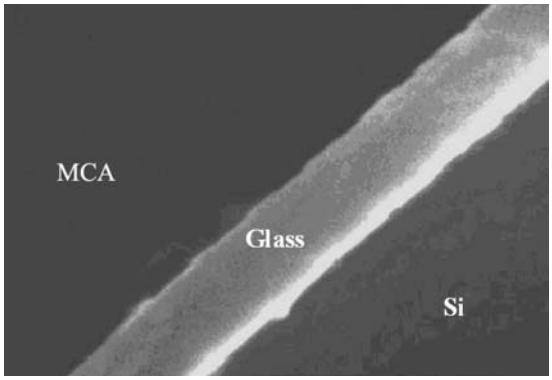

Fig. 3. SEM image of MCA/Si-wafer bonded infterface.

The reliability and possibility for applications of the MCA/Si wafer anodic-bonded sample are evaluated through the actuation test using laser displacement sensors (Sensing Part-AT0061, Deflection Analyzer-AT3700, Graphtec, Japan). The analysis of the deflection of Si diaphragms with various diaphragm thicknesses is shown in Fig. 4. With increasing diaphragm thickness to 400 μm, the maximum deflection in the center of the diaphragm decreased rapidly to 3.4 μm. On the basis of this result, it should be possible to accurately set the maximum deflection of an actuating part by fabricating a diaphragm of appropriate thickness.

The dimensions of Si diaphragms of 150 μm thickness are selected in the range of 9–18 mm^2. For Si diaphragms of various dimensions, the relationship between center deflection and applied voltage (DC 0–100 V) was measured using laser displacement sensors. All the diaphragms showed linear characteristics with increasing applied voltage to 100 V. Figure 5 shows the analysis of maximum deflection in the center of the Si diaphragm of different dimensions (9, 12, 15, 18 mm^2). With increasing diaphragm dimensions, the maximum deflection was measured to be from 11.16 to 13.2 μm. In spite of the different diaphragm dimensions, the nonlinearity was maintained at 0.05–0.08% FS. The hysteresis values were approximately 0.53–1.19% FS, and almost equal that of the displacement test that was reported by Furutani *et al.*[8] Also, during the actuation test, no damage or separation of the MCA/Si wafer bonded samples occurred.

Figure 6 shows a comparison of the experimental and expected values of maximum deflection for Si diaphragms of different dimensions. A solution of the deflection of the MCA/Si diaphragm structures is performed. It is assumed that the influence of the contact area between the MCA and Si diaphragm surface is negligible. The plate constant, D, is given as[9]

$$D = \frac{Et^3}{12\left(1-v^2\right)}, \tag{1}$$

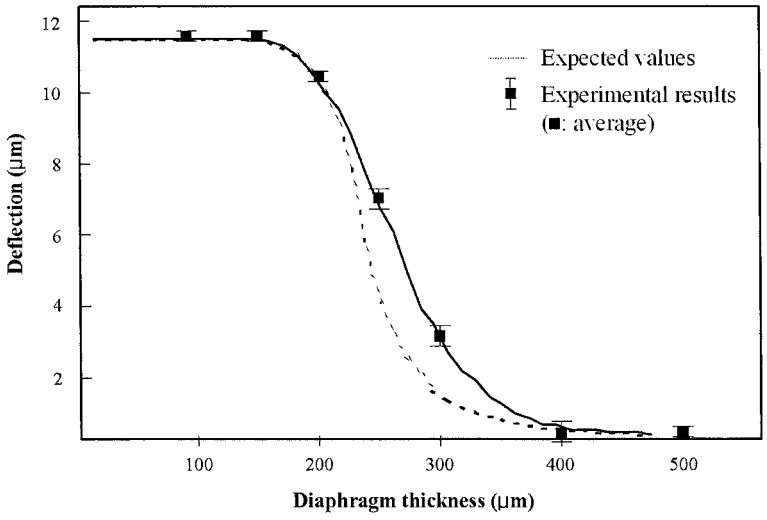

Fig. 4. Analysis of Si diaphragm deflection as function of diaphragm thickness.

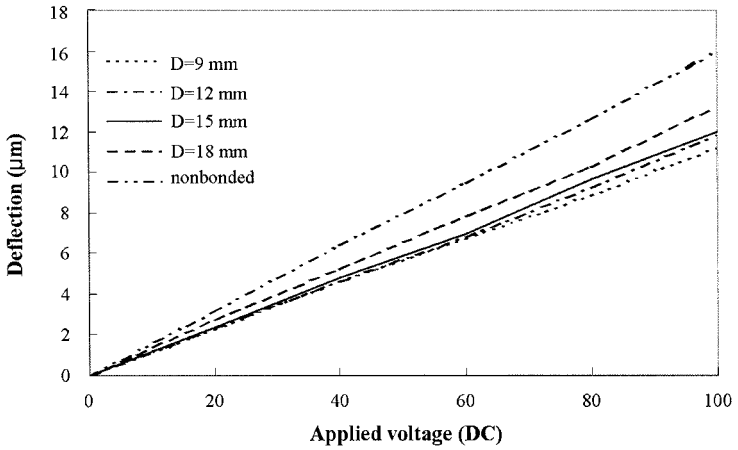

Fig. 5. Analysis of Si diaphragm deflection as function of applied voltage.

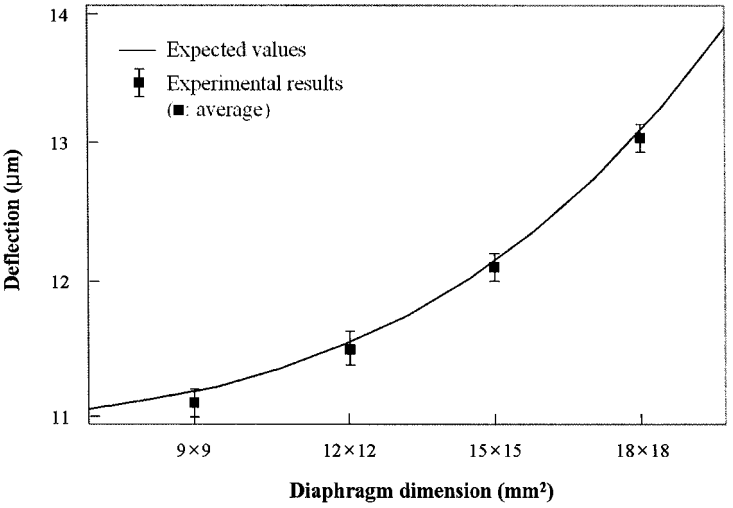

Fig. 6. Comparison of deflection predicted by analysis and experimental results obtained using laser displacement sensors.

where v, E and t are Poisson's ratio, Young's modulus and the Si diaphragm thickness, respectively. The analytical relation of diaphragm diameter and MLCA deflection is written as

$$d_{\max} = \frac{Pr^4}{48D}, \tag{2}$$

where P and r are the piezoelectric force and the diameter of the Si diaphragm, respectively. With increasing diaphragm diameter, the maximum deflection was measured to

range from 11.16 to 13.2 μm. Also, the maximum deflection distributions for all Si diaphragms were measured for the expected values as well.

To evaluate the Si-diaphragm-coupled MCA actuation, a finite element analysis (FEA) program was required. In this work, a simulation of the MCA/Si structure using ANSYS (solid 5 and solid 45) was performed. The thickness of the Si diaphragm was selected as 100–550 μm and the diameter of the Si diaphragm was 10 mm. A total of 6155 elements were employed. The deflection of the MCA/Si structures with Pyrex glass #7740 intermediate layer was modeled for when a voltage of 100 V was applied. Figure 7 shows

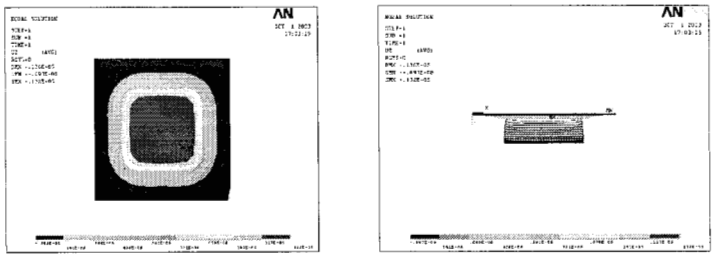

(a) 300 mm

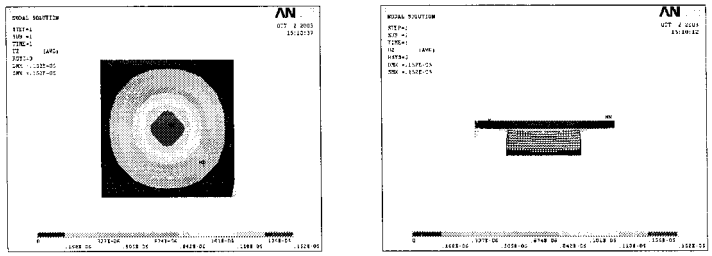

(b) 400 mm

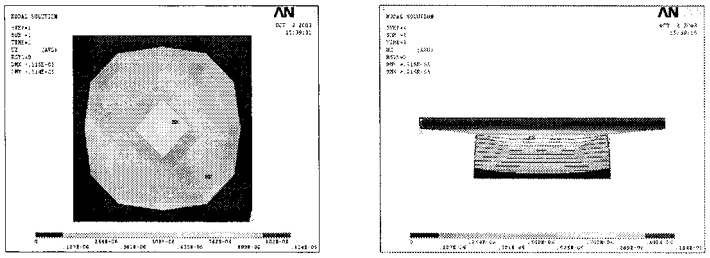

(c) 500 mm

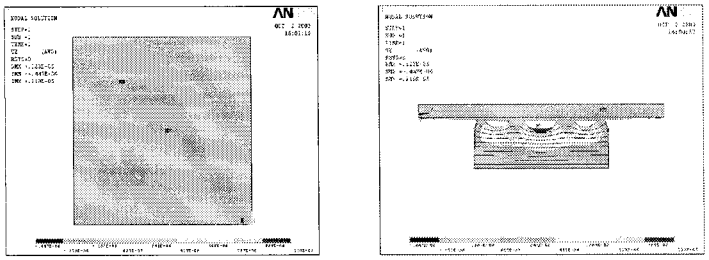

(d) 550 mm

Fig. 7. Simulation results of Si diaphragm deflection as function of diaphragm thickness.

simulation results of MCA deflection as functions of Si diaphragm thickness. MCA deflection at the center of the diaphragm is maintained at 13.8±0.1 μm up to a diaphragm thickness of 400 μm . In the case of a diaphragm thickness over 450 μm, partial separations occurred on the MLCA/Si diaphragm bonded surface and the maximum deflection is dramatically reduced to 0.241 μm.

An analytical comparison of the simulation and experiment results is shown in Fig. 8. With increasing diaphragm thickness up to 500 μm, the values of maximum deflection at the center of the diaphragm are markedly smaller than the simulation results. It looks as though material properties used in the simulation such as the Young's modulus of Si and the boundary conditions, were from the actual material properties. In addition, no damage or separation of MCA/Si anodic bonded samples occurred during the actuation test. On the basis of the experiment results, MCA/Si anodic bonding technology will require the fabrication of the actuating part using MCA/Si diaphragm structures, which have a good bond strength, a perfectly bonded area and accurate deflection control.

4. Conclusion

In this work, we have demonstrated successful bonding using sputtered Pyrex glass #7740 thin films for MEMS applications. In order to successfully test the MCA/Si anodic bonding, the optimum RF sputtering conditions to deposit Pyrex #7740 glass were determined to be an $Ar:O_2$ gas ratio of 100% and an input power of 1 W/cm^2. Using these deposited glasses, the MCA/Si samples were perfectly bonded by electrostatic forces without the presence of a nonbonded surface under the conditions of 400°C and 600 V. Also, we evaluated the linear characteristics and deflection distributions of MCA/Si bonded samples through the actuation test. For all diaphragms, which had a thickness of 150 μm and different dimensions (9–18 mm^2), we observed linear deflection characteristics as a function of applied voltage, which was gradually increased from 0 to 100 V. The maximum nonlinearity of deflection in diaphragms with different dimensions was 0.05–

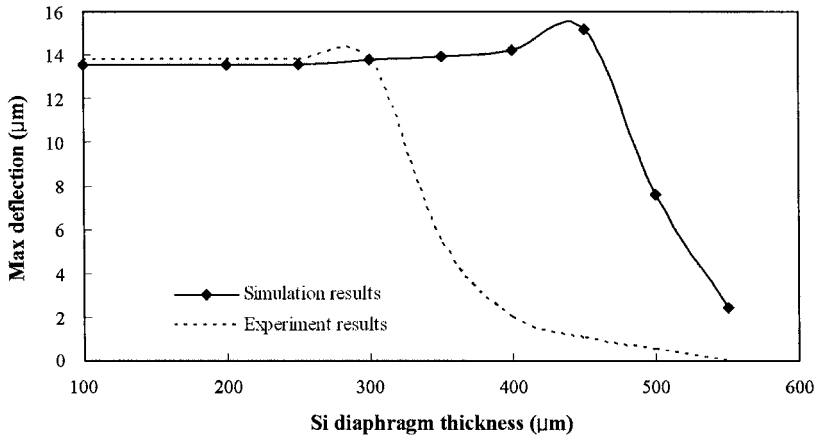

Fig. 8. Analysis of deflection of Si diaphragms as function of diaphragm thickness.

0.08% FS and the hysteresis was 0.53–1.19% FS. The maximum deflection distributions for Si diaphragms were measured for expected values as well. The deflection of MCA/Si diaphragms, which had different diaphragm thicknesses, was also simulated and measured. In the simulation results of a diaphragm of over 400 μm thickness, partial cracks occurred on the MCA/Si bonded surfaces. However, during the actuation test, separations of MCA/Si bonded samples were not observed. In conclusion, it is expected that the MCA/Si bonding process could be usefully applied to MEMS applications.

Acknowledgement

This research was supported by the 2004 Regional Industry R&D Project which was conducted by the Ministry of Industry and Energy of the Korean Government.

References

1 S. Weichel, R. Rous and M. Rindahl: Sensors and Actuators A **70** (1998) 179.
2 W. Zhu, K. Yao and Z. Zhang: Sensors and Actuators A **86** (2000) 149.
3 K. Tanaka, E. Tanaka and K. Ohwada: Sensors and Actuators A **69** (1998) 199.
4 G. Sasaki, H. Fukunaga, T. Suga and K. Tanaka: Materials Chemistry and Physics **51** (1997) 174.
5 T. Rogers and J. Kowal: Sensors and Actuators A **46** (1995) 113.
6 J. W. Berenschot, J. G. E. Gardeniers, T. S. J. Lammerink and M. Elwenspoek: Sensors and Actuators A **89** (1994) 338.
7 A. S. Sandhu and K. Singh: Radiation Physics and Chemistry **61** (2001) 579.
8 K. Furutani, M. Urushibata and N. Mohri: Nanotechology **9** (1998) 93 .
9 W. Wijngaart, H. Ask, P. Anoksson and G. Stemme: Sensors and Actuators A **100** (2002) 264.